General Disclaimer

One or more of the Following Statements may affect this Document

- This document has been reproduced from the best copy furnished by the organizational source. It is being released in the interest of making available as much information as possible.

- This document may contain data, which exceeds the sheet parameters. It was furnished in this condition by the organizational source and is the best copy available.

- This document may contain tone-on-tone or color graphs, charts and/or pictures, which have been reproduced in black and white.

- This document is paginated as submitted by the original source.

- Portions of this document are not fully legible due to the historical nature of some of the material. However, it is the best reproduction available from the original submission.

NASA TECHNICAL MEMORANDUM

NASA TM X-71841

NASA TM X-71841

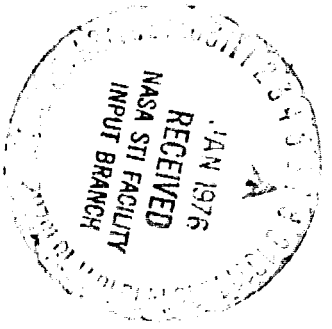

GRAVITATIONAL COLLAPSE OF A TURBULENT VORTEX WITH APPLICATION TO STAR FORMATION

by Robert G. Deissler
Lewis Research Center
Cleveland, Ohio 44135

TECHNICAL PAPER to be presented at
Fluid Dynamics Meeting sponsored by the
American Physical Society
College Park, Maryland, November 24-25, 1975

GRAVITATIONAL COLLAPSE OF A TURBULENT VORTEX WITH APPLICATION TO STAR FORMATION

by Robert G. Deissler
Lewis Research Center
Cleveland, Ohio 44135

E-8525

ABSTRACT

The gravitational collapse of a rotating cloud or vortex is analyzed by expanding the dependent variables in the equations of motion in two-dimensional Taylor series in the space variables. It is shown that the gravitation and rotation terms in the equations are of first order in the space variables, the pressure gradient terms are of second order, and the turbulent viscosity term is of third order. The presence of a turbulent viscosity insures that the initial rotation is solid-body-like near the origin. The effect of pressure on the collapse process is found to depend on the shape of the initial density disturbance at the origin. Dimensionless collapse times, as well as the evolution of density and velocity, are calculated by solving numerically the system of nonlinear ordinary differential equations resulting from the series expansions. The axial inflow plays an important role and allows collapse to occur even when the rotation is large. An approximate solution of the governing partial differential equations is also given, in order to study the spacial distributions of the density and velocity.

I. INTRODUCTION

Gravitational instabilities appear to play a dominant role in the formation of stars and other astronomical objects, and calculations of the gravitational collapse of clouds (protostars) have been carried out by a number of authors (e.g. Larson 1969, 1972, 1973; Disney et al. 1969; Penston 1971; Tscharnuter 1975). Most of these have been numerical solutions of the governing partial differential equations, where, except in recent work such as that of Larson (1972) and of Tscharnuter (1975), the effects of rotation have been neglected. But as will be seen, the effects of rotation are of the same order as those of gravity, and are of lower order than those of pressure gradients. In the past work boundary conditions were assumed at a hypothetical outer boundary, where conditions were generally not well known.

The present treatment differs from previous work in that the dependent variables are expanded about the origin in truncated power series in the space variables. This converts the governing partial differential equations to ordinary differential equations in time. Aside from the fact that the resulting ordinary differential equations are much easier to solve than are the original partial differential equations, this procedure has the advantage that the various physical processes are conveniently separated into first, second, and third order effects. Moreover the introduction of boundary conditions at an outer boundary is replaced by the natural assumption that the dependent variables and their lower order derivatives are finite at the origin. That is, the boundary conditions are applied at the origin, and we do not have to specify the extent of the gaseous cloud. However, we still have to specify the size of the initial disturbance.

The effects of pressure are included and are found to depend on the amplitude and shape of the initial disturbance. The effects of rotation and of turbulent viscosity are also included in the analysis. Although the quantitative effects of turbulent viscosity are only of third order, it appears that the presence of the turbulent viscosity is important for insuring that the velocity and its derivatives are bounded at the center of contraction and rotation.

Most of the calculations were carried out by using ordinary differential equations in the independent variable time, as described above. However, in some of the calculations the radius was also retained as a variable in order to investigate the spacial variations of density and velocity.

II. BASIC EQUATIONS

The equations of motion and continuity for an axially symmetric compressible flow can be written in cylindrical coordinates r, θ and z as

$$\frac{\partial u}{\partial t} = \frac{v^2}{r} - u\frac{\partial u}{\partial r} - w\frac{\partial u}{\partial z} - \frac{\partial \varphi}{\partial r} - \frac{1}{\rho}\frac{\partial p}{\partial r} \tag{1}$$

$$\frac{\partial v}{\partial t} = - u\frac{\partial v}{\partial r} - \frac{uv}{r} - w\frac{\partial v}{\partial z} - D \tag{2}$$

$$\frac{\partial w}{\partial t} = - w\frac{\partial w}{\partial z} - u\frac{\partial w}{\partial r} - \frac{\partial \varphi}{\partial z} - \frac{1}{\rho}\frac{\partial p}{\partial z} \tag{3}$$

and

$$\frac{\partial \rho}{\partial t} = - \frac{1}{r}\frac{\partial}{\partial r}(r\rho u) - \frac{\partial}{\partial z}(\rho w) \tag{4}$$

where the gravitational potential φ is given by the Poisson equation

$$\nabla^2\varphi = \frac{1}{r}\frac{\partial}{\partial r}\left(r\frac{\partial\varphi}{\partial r}\right) + \frac{\partial^2\varphi}{\partial z^2} = 4\pi G\rho \tag{5}$$

and where u, v, and w are the velocity components in the r, θ and z directions respectively, t is the time, ρ is the density, p is the pressure, G is the gravitational constant, and D is a turbulent or viscous drag term in the θ direction. Drag terms are not shown in equations (1) and (3) because those terms have been assumed small compared with (or included in) the pressure gradient terms. To relate the pressure to the density, we use the polytropic relation

$$p = p_1\rho_1^{-\gamma}\rho^{\gamma} \tag{6}$$

or

$$\frac{\partial p}{\partial r} = \gamma p_1\rho_1^{-\gamma}\rho^{\gamma-1}\frac{\partial\rho}{\partial r} \tag{6a}$$

where γ (assumed constant) is the polytropic exponent for the collapse process. The subscripts one designate ambient values.

The drag term D arises mainly because of the effects of turbulence, the effect of molecular viscosity usually being comparatively small for the high Reynolds numbers in astronomical systems. For our present purposes it should be sufficiently accurate to represent the effects of turbulence by a uniform turbulent viscosity ϵ as in Deissler and Perlmutter (1960). Thus we write

$$D = -\epsilon\left[\frac{\partial}{\partial r}\left(\frac{\partial v}{\partial r} - \frac{v}{r}\right) + \frac{2}{r}\left(\frac{\partial v}{\partial r} - \frac{v}{r}\right)\right] \tag{7}$$

In Deissler and Perlmutter it is supposed that ϵ is determined by the shear, and an estimate of its value is given by using a modification of

von Karman's similarity theory. It is shown there that for v proportional to r^{-1} (large radial flow)

$$\epsilon = \frac{\kappa^2}{2} r_1 v_1 \tag{8}$$

where κ is the Karman constant, and r_1 and v_1 are respectively the radius and tangential velocity at the outer edge of an initial disturbance to be specified. From the experiments cited in Deissler and Perlmutter,

$$\kappa^2/2 \approx 1/20 \tag{9}$$

In the present case, v lies between values given by an r^{-1} and an r variation, so that ϵ as determined by shear will tend to be lower than the value given by equation (8). We will retain equation (8) in the present study as an upper limit for ϵ as determined by shear. Other effects such as normal strain (Deissler 1968, 1972) and gravitational instabilities will tend to offset the decrease in ϵ associated with decreased shear, so that equation (8) may give a reasonable estimate. As will be shown, the effects of turbulent viscosity are quite small so that the exact value used for ϵ is not critical.

The set of equations (1) to (9) is determinate, and its solution will be considered in the next section.

III. SOLUTION BY TAYLOR SERIES

We can expand the dependent variables, u, v, w, ρ and φ (represented by χ) in two-dimensional Taylor series about $r = z = 0$, truncated after terms of third order in r and z, as

$$\chi = \chi_0 + \chi_r r + \chi_z z + \frac{1}{2}\chi_{rr} r^2 + \chi_{rz} rz + \frac{1}{2}\chi_{zz} z^2$$

$$+\frac{1}{6}\chi_{rrr}r^3+\frac{1}{2}\chi_{rrz}r^2z+\frac{1}{2}\chi_{rzz}rz^2+\frac{1}{6}\chi_{zzz}z^3 \tag{10}$$

where

$$\chi_0=(\chi)_{\substack{r=z\\=0}},\quad \chi_r=\left(\frac{\partial\chi}{\partial r}\right)_{\substack{r=z\\=0}},\quad \chi_{rz}=\left(\frac{\partial^2\chi}{\partial r\,\partial z}\right)_{\substack{r=z\\=0}},\quad \text{etc.}$$

We take the r and z axes as axes of symmetry, so that the dependent variables are symmetric or antisymmetric about those axes. Then (see Fig. 1)

$$u(r,-z)=u(r,z) \qquad w(r,-z)=-w(r,z)$$

$$u(-r,z)=-u(r,z) \qquad w(-r,z)=w(r,z)$$

$$u(-r,-z)=-u(r,z) \qquad w(-r,-z)=-w(r,z)$$

$$\rho(r,-z)=\rho(r,z) \qquad \varphi(r,-z)=\varphi(r,z)$$

$$\rho(-r,z)=\rho(r,z) \qquad \varphi(-r,z)=\varphi(r,z)$$

$$\rho(-r,-z)=\rho(r,z) \qquad \varphi=(-r,-z)=\varphi(r,z)$$

The vortex rotates about z, so that

$$v(-r,z)=-v(r,z)$$

$$v(r,-z)=v(r,z)$$

$$v(-r,-z)=-v(r,z)$$

If we impose these symmetry conditions on equation (10), we get

$$u=u_r r+\frac{1}{6}u_{rrr}r^3+\frac{1}{2}u_{rzz}rz^2 \tag{11}$$

$$v=v_r r+\frac{1}{6}v_{rrr}r^3+\frac{1}{2}v_{rzz}rz^2 \tag{12}$$

$$w=w_z z+\frac{1}{2}w_{rrz}r^2z+\frac{1}{6}w_{zzz}z^3 \tag{13}$$

$$\rho=\rho_0+\frac{1}{2}\rho_{rr}r^2+\frac{1}{2}\rho_{zz}z^2 \tag{14}$$

$$\varphi = \varphi_0 + \frac{1}{2}\varphi_{rr}\, r^2 + \frac{1}{2}\varphi_{zz}\, z^2 \tag{15}$$

Consider first the gravitational potential φ. Substituting equations (14) and (15) in (5) gives, for coefficients of r^0

$$2\varphi_{rr} + \varphi_{zz} = 4\pi G\rho_0 \tag{16}$$

The relation between φ_{rr} and φ_{zz} can be considered as a boundary condition for φ. For that boundary condition we set $\varphi_{rr} = \varphi_{zz}$; that is we assume spherical symmetry for φ near the origin. Larson (1972) found that his results were not sensitive to the particular boundary conditions used for φ. Thus equation (16) becomes

$$\varphi_{rr} = \varphi_{zz} = \frac{4\pi}{3} G\rho_0 \tag{17}$$

From equations (15) and (17),

$$\frac{\partial\varphi}{\partial r} = \frac{4\pi}{3} G\rho_0 r \tag{18}$$

and

$$\frac{\partial\varphi}{\partial z} = \frac{4\pi}{3} G\rho_0 z \tag{19}$$

Substituting equations (11) to (14), (18) and (19) into equations (1) to (9), and equating the sums of the coefficients of like powers of r and z to zero gives the following system of nonlinear ordinary differential equations:

$$\frac{du_r}{dt} = v_r^2 - u_r^2 - \frac{4\pi}{3} G\rho_0 - \gamma p_1 \rho_1^{-\gamma} \rho_0^{\gamma-2} \rho_{rr} \tag{20}$$

$$\frac{dv_r}{dt} = -2u_r v_r + \frac{v_1 r_1}{15} v_{rrr} \tag{21}$$

$$\frac{dw_z}{dt} = -w_z^2 - \frac{4\pi}{3} G\rho_0 - \gamma p_1 \rho_1^{-\gamma} \rho_0^{\gamma-2} \rho_{zz} \tag{22}$$

$$\frac{d\rho_0}{dt} = -2\rho_0 u_r - \rho_0 w_z \tag{23}$$

$$\frac{d\rho_{rr}}{dt} = -\frac{4}{3}\rho_0 u_{rrr} - 4\rho_{rr} u_r - \rho_0 w_{rrz} - \rho_{rr} w_z \tag{24}$$

$$\frac{d\rho_{zz}}{dt} = -2\rho_0 u_{rzz} - 2\rho_{zz} u_r - \rho_0 w_{zzz} - 3\rho_{zz} w_z \tag{25}$$

$$\frac{du_{rrr}}{dt} = 2v_r v_{rrr} - 4u_r u_{rrr} - 3\gamma(\gamma-2)p_1\rho_1^{-\gamma}\rho_0^{\gamma-3}\rho_{rr}^2 \tag{26}$$

$$\frac{du_{rzz}}{dt} = 2v_r v_{rzz} - 2u_r u_{rzz} - 2w_z u_{rzz} - \gamma(\gamma-2)p_1\rho_1^{-\gamma}\rho_0^{\gamma-3}\rho_{rr}\rho_{zz} \tag{27}$$

$$\frac{dv_{rrr}}{dt} = -4u_r v_{rrr} - 2v_r u_{rrr} \tag{28}$$

$$\frac{dv_{rzz}}{dt} = -2u_r v_{rzz} - 2v_r u_{rzz} - 2w_z v_{rzz} \tag{29}$$

$$\frac{dw_{rrz}}{dt} = -2u_r w_{rrz} - 2w_z w_{rrz} - \gamma(\gamma-2)p_1\rho_1^{-\gamma}\rho_0^{\gamma-3}\rho_{rr}\rho_{zz} \tag{30}$$

$$\frac{dw_{zzz}}{dt} = -4w_z w_{zzz} - 3\gamma(\gamma-2)p_1\rho_1^{-\gamma}\rho_0^{\gamma-3}\rho_{zz}^2 \tag{31}$$

The set of equations (20) to (31) results from retaining terms through third order in r and z in equations (11) to (14), (18) and (19). That is, equations (20) to (31) form a third order set of equations. If, on the other hand, we retain only terms of first order in r and z, we get the following first-order set:

$$\frac{du_r}{dt} = -u_r^2 + v_r^2 - \frac{4\pi}{3}G\rho_0 \tag{32}$$

$$\frac{dv_r}{dt} = -2u_r v_r \tag{33}$$

$$\frac{dw_z}{dt} = -w_z^2 - \frac{4\pi}{3} G\rho_0 \tag{34}$$

$$\frac{d\rho_0}{dt} = -2\rho_0 u_r - \rho_0 w_z \tag{35}$$

If we retain terms through second order in equations (11) to (14), (18), and (19), we get the following second-order set of equations:

$$\frac{du_r}{dt} = v_r^2 - u_r^2 - \frac{4\pi}{3} G\rho_0 - \gamma p_1 \rho_1^{-\gamma} \rho_0^{\gamma-2} \rho_{rr} \tag{36}$$

$$\frac{dv_r}{dt} = -2u_r v_r \tag{37}$$

$$\frac{dw_z}{dt} = -w_z^2 - \frac{4\pi}{3} G\rho_0 - \gamma p_1 \rho_1^{-\gamma} \rho_0^{\gamma-2} \rho_{zz} \tag{38}$$

$$\frac{d\rho_0}{dt} = -2\rho_0 u_r - \rho_0 w_z \tag{39}$$

$$\frac{d\rho_{rr}}{dt} = -4\rho_{rr} u_r - \rho_{rr} w_z \tag{40}$$

$$\frac{d\rho_{zz}}{dt} = -2\rho_{zz} u_r - 3\rho_{zz} w_z \tag{41}$$

Several interesting observations can be made by comparison of the first, second, and third order sets of equations. Examination of the first order set (eqs. (32) to (35)) shows that gravitational and rotational forces (last two terms in eq. (32) and last term in (34)) appear when first-order terms are retained in the series expansions in r and z. The second-order set (eqs. (36) to 41)) contains in addition, pressure gradient terms

(last terms in eqs. (36) and (38)). Finally, if third-order terms are retained in the series expansions (eqs. (20) to (31)), a turbulent viscosity term appears (last term in eq. 21)). Another way of saying this is that gravitational and rotational terms appear in the equations when only first spacial derivatives (u_r, v_r, and w_r) are present at the origin, pressure gradient effects require, in addition, second spacial derivatives (ρ_{rr} and ρ_{zz}), and turbulent viscosity effects require the presence of the third spacial derivative v_{rrr} at the origin.

Before we can solve the set of equations (20) to (31) numerically, we must set conditions at an initial time, say at $t = 0$. We set the initial radial and axial flows equal to zero in the vicinity of the origin, so that

$$u_r^0 = u_{rrr}^0 = u_{rzz}^0 = w_z^0 = w_{rrz}^0 = w_{zzz}^0 = 0 \tag{42}$$

where the superscripts zero indicate values at $t = 0$. Also we take the angular velocity $\omega = v_r$ as initially uniform near the origin, so that

$$v_r^0 = \omega^0 \tag{43}$$

and

$$v_{rrr}^0 = v_{rzz}^0 = 0 \tag{44}$$

Finally, we specify the initial density in the vinicity of the origin. For doing this, we introduce an initial disturbance of radius r_1 such that for $z = 0$,

$$\rho^0 = \Delta\rho^0\left[1 - \left(\frac{r}{r_1}\right)^n\right]^2 + \rho_1 \tag{45}$$

and for $r = 0$,

$$\rho^0 = \Delta\rho^0\left[1 - \left(\frac{z}{r_1}\right)^n\right]^2 + \rho_1 \tag{46}$$

where $\Delta\rho^0$ is the magnitude of the initial density fluctuation at the origin and n is an integer ≥ 2. This initial density distribution is convenient, since its shape at the origin can be altered by varying n, and since it gives the ambient density ρ_1 at r_1. Moreover it gives zero density gradient where the density becomes ambient at r_1, so that the distribution given by equations (45) and (46) joins smoothly with the uniform ambient distribution outside of r_1. For $r = z = 0$,

$$\rho^0 = \rho_0^0 = \Delta\rho_0^0 + \rho_1 \tag{47}$$

and

$$\rho_r^0 = 0$$

in agreement with equation (14). Taking the second derivatives of equations (45) and (46) and setting $r = z = 0$, we get

$$\rho_{rr}^0 = \rho_{zz}^0 = -4\frac{\Delta\rho^0}{\rho_1} \quad \text{for} \quad n = 2 \tag{48}$$

and

$$\rho_{rr}^0 = \rho_{zz}^0 = 0 \quad \text{for} \quad n > 2 \tag{49}$$

IV. NUMERICAL RESULTS AND DISCUSSION

The set of equations (20) to (31) was solved numerically, subject to the initial conditions at $t = 0$ given by equations (42) to (49). Before carrying out the solution, the equations and initial conditions were converted to dimensionless form. For example, equation (20) can be written as

$$\frac{du_r^*}{dt^*} = v_r^{*2} - u_r^{*2} - \frac{4\pi}{3} G^* \rho_0^* - \gamma p_1^* \rho_0^{*\gamma-2} \rho_{rr}^* \tag{50}$$

where

$$u_r^* = \frac{u_r}{\omega^0}, \quad v_r^* = \frac{v_r}{\omega^0}$$

$$t^* = \omega^0 t, \quad \rho_0^* = \frac{\rho_0}{\rho_1}$$

$$G^* = \frac{G\rho_1}{\omega^{0^2}}, \quad p_1^* = \frac{p_1}{\rho_1 r_1^2 \omega^{0^2}}$$

$$\rho_{rr}^* = \frac{r_1^2 \rho_{rr}}{\rho_1}$$

Similar dimensionless equations are obtained from equations (21) to (31) and the initial conditions. As before, the superscripts zero indicate values at $t = 0$, the subscripts zero indicate values at $r = z = 0$, and the subscripts one designate constant ambient values. Thus the dimensionless dependent variables can be written as functions of a dimensionless time, a gravitational parameter, and a pressure parameter. That is,

$$u_r^* = f(t^*, G^*, p_1^*) \tag{51}$$

Similar equations are obtained for the other dependent variables. Dimensionless quantities other than those in equation (51) can, of course, be used in their place, so long as the same total number of variables appears on the right side. For instance by intermultiplying t^*, G^* and p_1^*, we get

$$G^{1/2}\rho_1^{1/2}t = G^{*1/2}t^*, \quad \frac{\omega^0}{G^{1/2}\rho_1^{1/2}} = \frac{1}{G^{*1/2}}$$

and

$$\frac{p_1}{G\rho_1^2 r_1^2} = \frac{p_1^*}{G^*}$$

so that in place of equation (51) we have

$$\frac{u_r}{\omega^0} = f\left(G^{1/2}\rho_1^{1/2}t, \ \frac{\omega^0}{G^{1/2}\rho_1^{1/2}}, \ \frac{p_1}{G\rho_1^2 r_1^2}\right) \tag{52}$$

When written this way, we can think of the dependent variables as funtions of a dimensionless time, a rotational parameter, and a pressure parameter. Note that in equation (52) the rotation is confined to one parameter, in contrast to equation (51) where, instead, gravity occurs in only one parameter. In both cases the pressure is confined to one parameter.

a) Uniform Initial Density Distribution

Consider first the case where the initial disturbance at the origin $\Delta\rho^0$ is zero (see eqs. (45) and (46)). That is, the density is initially uniform as in Larson's (1972) rotating case. However, the present case differs from that of Larson because he assumed that the radial velocity remains zero at an outer boundary. For $\Delta\rho^0 = 0$, equations (48) and (49) indicate $\rho_{rr} = \rho_{zz} = 0$ initially, regardless of the value of n in equations (45) and (46). But if ρ_{rr} and ρ_{zz}, as well as the radial velocity are initially zero near the origin (eq. (42)), equations (20) to (31) indicate that those quantities will remain zero. Numerical solution of

the equations confirmed this; small disturbances (round off errors) did not grow with time. Thus, if the initial density is uniform ($\Delta\rho^0 = 0$), the pressure and turbulent viscosity terms in equations (20) to (31) will be zero at all times, and the equations reduce to the first-order set given by equations (32) to (35).

Calculated results for an initially uniform density are plotted in figures 2 to 4. A modified Gear method (Windmarsh 1974) was used for the numerical computations. In agreement with the preceding discussion the results are independent of pressure-gradient and turbulent viscosity effects. This is true regardless of the value of the polytropic exponent γ. The density changes comparatively slowly over a considerable time span and then begins to change rapidly. For each value of the rotation parameter there is a particular dimensionless time, designated the collapse time, for which the density and other dependent variables at the origin increase without limit. That is, the rotating cloud or vortex tends to collapse at that time to form a star. The collapse time increases with angular velocity ω because the centrifugal field produced by the rotation tends to prevent collapse.

Another effect of the rotation is that for large initial angular velocities ω^0, the density at the center ρ_0 can decrease before it increases, as in figure 2. This is again because of the centrifugal field associated with the rotation which tends to throw the gas outward, in opposition to the gravitational field. Figure 4 shows that for the larger dimensionless angular velocity, the radial flow near the center is outward (u_r is positive) until shortly before the collapse time. On the other hand the flow near the center in the axial direction (z-direction) is always inward

(w_z is negative) because of gravitational attraction and the absence of centrifugal effects in the axial direction. This inward axial flow is in fact the main reason that collapse can eventually occur even when the radial flow is outward for awhile. When the radial flow is outward, the angular velocity at the origin ω decreases with time as in figure 3. This decreases the centrifugal force field so that the radial flow can become negative (u_r becomes negative), and collapse eventually occurs. But if it were not for the axial inflow during this time, the gravitational field would be weakened to such an extent because of the decreased density, that collapse would not occur. Although figure 2 indicates that the density at the origin ρ_0 can decrease because of the radial outflow, that decrease is not nearly as great as is would be if the axial inflow were absent. Thus, the collapse process for a rotating cloud can be much more complicated that it is for $\omega = 0$.

In order to investigate the spacial variations of the density and velocity, and to give somewhat more confidence in the series solution for $r = z = 0$ plotted in figures 2 to 4 an approximate numerical solution of the original partial differential equations was obtained. To reduce the number of independent spacial variables to one, and thus to hold the required computation time within reasonable limits, the solution was obtained for $z = 0$. Then $w = 0$, and we set

$$\frac{\partial}{\partial z}(\rho w) = \rho\frac{\partial w}{\partial z} \approx \frac{\rho u}{r}\frac{(\partial w/\partial z)_{r=z=0}}{(\partial u/\partial r)_{r=z=0}} \tag{53}$$

in equation (4), where ρ had been taken outside of the derivative sign because, by symmetry, $\partial\rho/\partial r = 0$ at $z = 0$. Equation (53) is exact if the

flow toward or away from the origin is spherically symmetric ($(\partial w/\partial z)_{r=z=0} = (\partial u/\partial r)_{r=z=0}$). It also gives a consistent result for $r = z = 0$ for spherically nonsymmetric flow, since (equation (11)) u/r approaches $\partial u/\partial r$ at the origin. Finally it is consistent for no axial flow ($\partial w/\partial z = 0$). For $(\partial w/\partial z)_{r=z=0}$ in equation (53) we use equation (34) since, as mentioned previously, equation (22) reduces to that equation for uniform initial density. We take the gravitational potential φ as spherically symmetric in order to give results consistent with those for the series solution. (In the series solution φ was taken to be spherically symmetric at the origin (eq. (17)). Again we note that Larson's (1972) work indicates that this assumption should give good results. Equation (5) gives, for φ spherically symmetric,

$$\frac{\partial \varphi}{\partial r} = 4\pi \frac{G}{r^2} \int_0^r \rho(\xi)\xi^2 d\xi \tag{54}$$

As in the case of the series solution we apply all of the boundary conditions at the origin. Equations (11) to (14) show that we can use for boundary conditions, $u = v = w = \partial^2 v/\partial r^2 = \partial \rho/\partial r = 0$, at $r = z = 0$.

Equations (1), (2), (4), (6) to (9), (34), (53) and (54) were solved numerically by an improved Euler method with increments for r/r_1 of 0.01, except near $r = 0$ where increments of 0.005 were used. To give results comparable with those for the series solution in figures 2 to 4, the density and angular velocity were taken as initially uniform, and u as initially zero. (For the series solution those initial conditions were applied only in the vicinity of $r = z = 0$). Results for $\omega^0/\left(G^{1/2}\rho_1^{1/2}\right) = 1$, $p_1/\left(G\rho_1^2 r_1^2\right) = 0.1$, and $\gamma = 5/3$ are plotted against r/r_1 in figures 5 to 7.

For comparison with the series solution, densities at $r = z = 0$ are also plotted in figure 2. The agreement is satisfactory.

Figure 5 shows that the vortex collapses in a nonhomologous (non-similar) fashion in agreement with the results of Larson (1972). A difference between our results and those of Larson is that the latter showed the formation of a ring of mass for rotating flow, rather than a concentration at the center. (It will be seen later however that our results for $\Delta\rho^0 < 0$ are somewhat similar to Larson's results.) It is not clear whether this difference is due to a difference in boundary conditions (Larson assumed $u = 0$ at an outer boundary), to the numerical techniques used, or to the inclusion of turbulent viscosity effects (with $v = \partial^2 v/\partial r^2 = 0$ at the center) in the present calculations. It is of interest that Tscharnuter (1975), using conditions similar to those of Larson, but a numerical technique differing from both that of Larson and the present paper, obtained a concentration of mass at the center.

The density distributions in figure 5 remain flat near the center of the vortex. This flatness is a carry over from the initially uniform density distribution. It is in agreement with equations (24), (26), (28) and (30), which show that for uniform initial ρ, u, w, and ω, ρ will remain uniform near the origin (ρ_{rr} remains zero), as discussed earlier. Also figures 6 and 7 show that v and u remain linear near the origin, as they should if the first-order set of equations (32) to (35) is to give a description of the collapse process. (As discussed previously, the set of equations (20) to (31) reduce to the set (32) to (35) in the present case.)

Figures 6 and 7 show that the variations of u and v with r are nearly linear for a considerable time span (beginning at $t = 0$). In the

case of u this is partly because, for a slowly varying density, the gravitational force is nearly linear in r (eq. (54)). The only other term in equation (1) which is important at early times is the v^2/r term, which is also nearly linear in r. Thus for early times with $\rho = \rho_1$, equation (1) integrates to

$$u = \left(\omega_0^2 - \frac{4\pi}{3} G\rho_1\right) rt \tag{55}$$

and equation (2) gives

$$v = \left[1 + \left(\frac{4\pi}{3} G\rho_1 - \omega_0^2\right) t^2\right] \omega_0 r \tag{56}$$

both of which are linear in r. For larger times the variations of u and v become highly nonlinear and tend to develop peaks. In the case of u this is evidently because the mass becomes concentrated near the origin and the gravitational force is nearly proportional to r^{-2} outside of the mass concentration. Inside of the mass concentration the density is uniform so that the gravitational force, and thus u, are still proportional to r. The peakedness of the v profiles in the vicinity of the peaks of the u curves is due to the fact that for large u, v approaches a 1/r variation (invicid vortex solution).

To determine the effect of turbulent viscosity on the results, curves for that quantity set equal to zero are plotted dashed in figure 6 for comparison with the curves for nonzero turbulent viscosity. The differences are slight. In particular the good agreement near the origin indicates that the effect of turbulent viscosity on the angular velocity at the origin ($\omega = v_r$) is zero. This is in agreement with the series solution, where the turbulent viscosity term drops out for the present case (uniform

initial ρ). For times larger than those shown, the effect of turbulent viscosity in the vicinity of the peak may become greater, but the effect on the angular velocity at the origin should still be zero.

The result that the turbulent viscosity has no effect on the angular velocity at the origin may seem to be contrary to experience. For instance when the arms of a whirling skater are retracted or extended they exert a tangential force on the skater's trunk and thus change the angular velocity of the latter. In that case the tangential force is necessary for changing the angular velocity of the trunk. The difference between that case and the rotating cloud (where a tangential force or turbulent viscosity is not necessary) appears to be that in the latter the radial velocity extends all the way to the center and is zero only at the center. In order to check a case which was comparable to that of the skater, u was set equal to zero for r/r_1 between 0 and 0.1. It was found that the angular velocity at the center changed with time only when the turbulent viscosity was nonzero.

Perhaps the most important effect of turbulent viscosity is that it enables the assumed initial solid-body-like rotation to be realized. In the absence of a turbulent viscosity the v profile could be arbitrary, and there would be no assurance that y and its spacial derivatives are finite at the origin, as required for the series solution. The presence of the eddy viscosity however provides a tangential stiffness, so that the assumed wheel flow can be attained, particularly near the origin. Figure 6 and equation (56) show that once an initial wheel flow is established, it can remain for a considerable time, even in the presence of small radial flows.

b) Nonuniform Initial Density Distributions

Consider first the case where $\Delta\rho^0 \neq 0$ and $n > 2$ in equations (45) and (46). Then equation (49) shows that ρ_{rr} and ρ_{zz} are initially zero, and equations (20) to (31) show that they will remain zero for the initial conditions used herein. Thus, as in the case of $\Delta\rho^0 = 0$, the set of third-order equations (20) to (31) reduces to the first-order set (32) to (35). The results for this case will therefore be similar to those for uniform initial density at the origin, although ρ_0^0 will be different (for the same ambient density ρ_1). The discussion for uniform initial density applies to the non-uniform case when $n > 2$ in equations (45) and (46), at least to the present order of approximation. Density evolution curves for $\Delta\rho^0/\rho_1 = 0.1 \left(\rho_0^0/\rho_1 = 1.1\right)$ are plotted in figure 8. As expected, these curves, as well as those for the velocity components (not shown), are similar to those for $\Delta\rho^0/\rho_1 = 0$. They are independent of pressure and the polytropic exponent γ.

Dimensionless collapse times for various values of rotation parameter and $\Delta\rho^0/\rho_1$ are plotted in figure 9. We note that the curves for $\Delta\rho^0 \neq 0$ could be obtained by multiplying the ordinates on the latter by $\left(1 + \Delta\rho^0/\rho_1\right)^{-1/2}$ and the abscissas by $\left(1 + \Delta\rho^0/\rho_1\right)^{1/2}$. The collapse times are of the same order of magnitude as the free-fall times, in agreement with the results of Larson and others.

To determine the effect of a non-uniform initial density profile on the profiles at later times, the governing partial differential equations were solved by the method and approximations used for the uniform initial density case in figure 5. The results are shown in figure 10, where ρ/ρ_1 is plotted against r/r_1 for various dimensionless times, and for $n = 4$

and $\Delta\rho^0/\rho_1 = \pm 0.1$ in equations (45) and (46). The rest of the parameters are the same as those in figure 5. Comparison of figures 5 and 10 indicates that the initial density profile can have a large effect on the evolution of the profiles. In particular the curves for $\Delta\rho^0/\rho_1 = -0.1$ (Fig. 10(b)) show the development of a pronounced peak away from $r = 0$. These profiles are somewhat similar to those of Larson (1972) for rotating flow and uniform initial density. In the present case the effect does not seem to be entirely due to rotation, because when v was set equal to zero, the curves, although considerably altered, still showed the development of a peak away from $r = 0$. This concentration of mass in a ring may break up into a binary star system (Larson, 1972). For all three cases the values of $\partial^2\rho/\partial r^2$ at $r = 0$ remained zero, as they should according to the series solution for these cases.

We still have to consider the case where $n = 2$, $p_1 > 0$, and $\Delta\rho^0 \neq 0$ in equations (45) and (46). This is the only case for which ρ_{rr} and ρ_{zz}, according to the present third-order solution, are not equal to zero, so that we have to consider the full set of equations (20) to (31). The pressure and the polytropic exponent γ, as well as the turbulent viscosity, may have an effect on quantities at $r = z = 0$ for this case.

Results for $n = 2$, $p_1/\left(G\rho_1^2 r_1^2\right) = 1$, $\Delta\rho^0/\rho_1 = \pm 0.1$, and $\gamma = 1$ and 5/3 are plotted in figure 11. First, second, and third order approximations for the evolution of densities at the origin are shown. (For the previous cases where $n > 2$ or $\Delta\rho^0 = 0$, the three approximations were of course identical.) The fact that the second and third order approximations are nearly the same, particularly for $\gamma = 1$ (optically thin case), indicates that the third order approximation gives quite accurate results. The dashed curves for the first approximation are also the curves for zero

pressure (zero temperature for nonzero density) for the three approximations. Results for small pressures were essentially the same as those for zero pressure, indicating that the results for zero pressure are stable. The effect of pressure for positive $\Delta\rho^0$ is to slow up the collapse process, since the pressure-gradient force is away from the center. (The pressure gradient is in the same direction as the density gradient, according to eq. (6a).) For negative $\Delta\rho^0$ the opposite trend occurs. Increasing the value of γ or of $\Delta\rho^0$ amplifies these effects. Tne turbulent viscosity term in equation (21), a third-order term, was found to be negligibly small in most cases.

The solid curve for $\gamma = 5/3$ in figure 11(a) indicates that contraction stops after a maximum density is reached. The curves for $\gamma = 1$, as well as those for $\gamma = 5/3$ in figure 11(b), however, show a strong tendency for collapse to continue. In the latter cases the gravitational force apparently increases faster than the resisting (for positive $\Delta\rho^0$) pressure-gradient force. These trends, except those for $\gamma = 5/3$ and a negative $\Delta\rho^0$ in figure 11(b), are in agreement with simplified analyses which indicate that only for $\gamma < 4/3$ will collapse occur (e.g. Schatzman 1972). For a negative $\Delta\rho^0$ the pressure-gradient force can aid, rather than hinder the collapse process so that it does not seem surprising that there can be a strong tendency for collapse to occur in that case, even for $\gamma = 5/3$. Of course as discussed earlier, for uniform initial density ($\Delta\rho^0 = 0$), or for $n > 2$ in equations (45) and (46), that is, if $\partial^2\rho/\partial r^2$ at the center is initially zero or negligibly small, our series solution indicates that collapse can occur regardless of the values of γ and of pressure parameter. Thus if the initial disturbance can be approximated

by equations (45) and (46) the pressure and γ, according to the present third order analysis, should have an effect on the collapse process at the origin only for a rather special case, that is, for $n = 2$ and $\Delta\rho \neq 0$.

I should like to acknowledge the work of Frank Molls on the numerical solutions of the differential equations in the present paper.

REFERENCES

1. Deissler, R. G. and Perlmutter, M. 1960, Int. J. Heat Mass Transfer, 1, 173.
2. Deissler, R. G. 1968, ZAMM, 48, 87.
3. Deissler, R. G. 1972, Phys. Fluids, 15, 1918.
4. Disney, M. F., and McNally, D., and Wright, A. E. 1969, Mon. Not. R. Astr. Soc., 146, 123.
5. Hindmarsh, A. E. and G lin.s, R. G. 1974, Lawrence Livermore Lab. Rept. UCID-30001.
6. Larson, R. B. 1969, Mon. ot. R. Astr. Soc., 145, 271.
7. Larson, R. B. 1972, M .. Not. R. Astr. Soc., 156, 437.
8. Larson, R. B. 1973, in Ann. Review of Astronomy and Astrophysics, Vol. 11, p. 219.
9. Penston, M. V. 1971, Contem. Phys., 12, 379.
10. Schatzman, E. 1972, Physics of the Solar System, ed. S. I. Rasool NASA SP-300, p. 409.
11. Tscharnuter, W. 1975, Astronomy and Astrophysics, 39, 207.

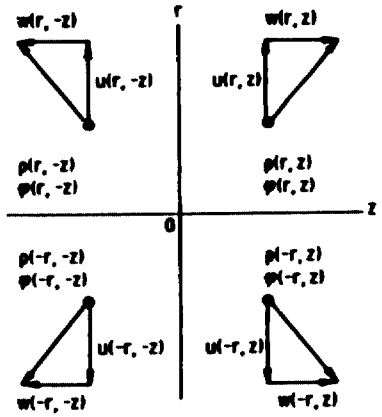

Figure 1. - Sketch showing symmetry conditions.

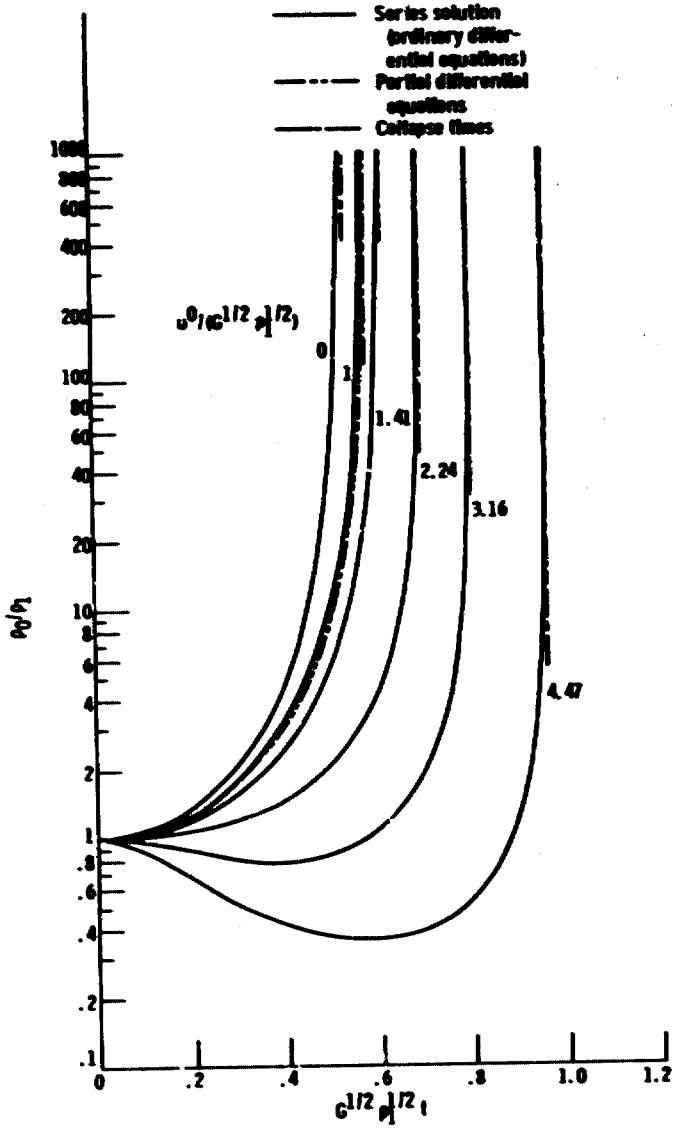

Figure 2. - Time evolution of density at center of vortex for various values of rotation parameter. Density and angular velocity near center are initially uniform, and radial and axial velocities near center are initially zero. Results are independent of pressure, polytropic exponent, and turbulent viscosity effects.

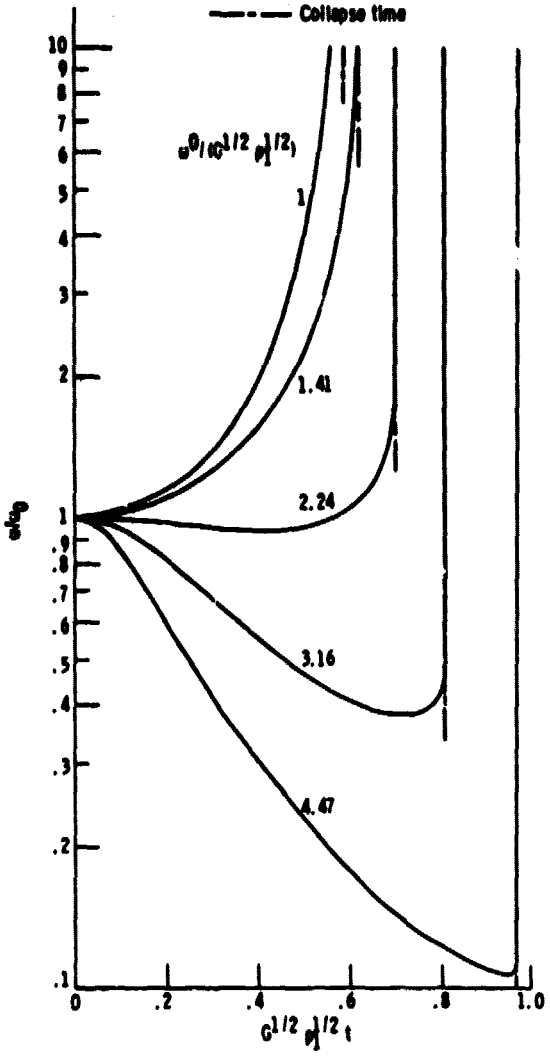

Figure 3. - Time evolution of angular velocity at center of vortex for various values of rotation parameter. Density and angular velocity near center are initially uniform, and radial and axial velocities near center are initially zero. Results are independent of pressure, polytropic exponent, and turbulent viscosity effects.

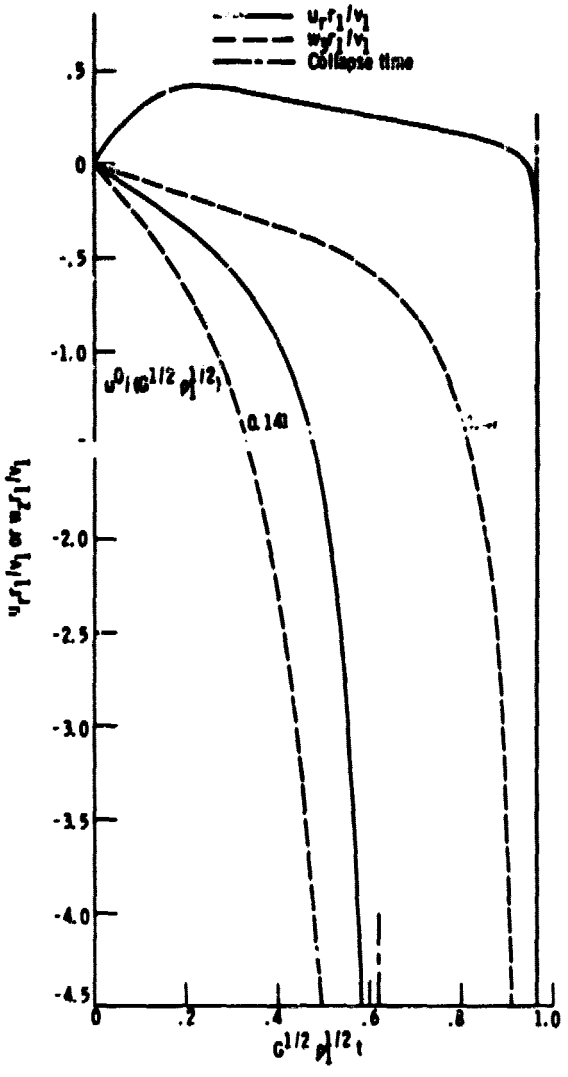

Figure 4. - Time evolution of radial and axial velocity derivatives at center of vortex for various values of rotation parameter. Density and angular velocity near center are initially uniform, and radial and axial velocities near center are initially zero. Results are independent of pressure, polytropic exponent, and turbulent viscosity effects.

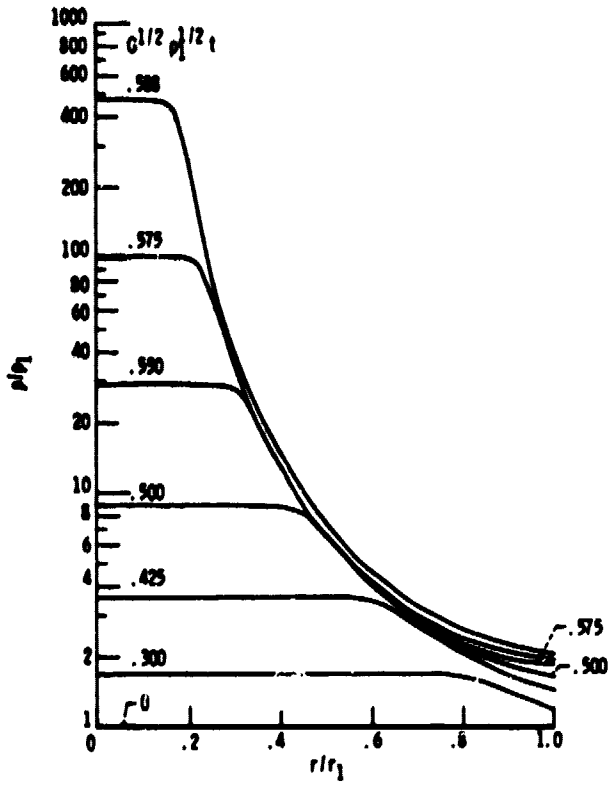

Figure 5. - Development of density profile in vortex. $u^0/(G^{1/2}\rho_1^{1/2}) = 1$. $p_1/(G\rho_1^2 r_1^2) = 0.1$. $\gamma = 5/3$. Density and angular velocity are initially uniform, and radial and axial velocities are initially zero. Results near center of vortex are independent of pressure, polytropic exponent, and turbulent viscosity effects.

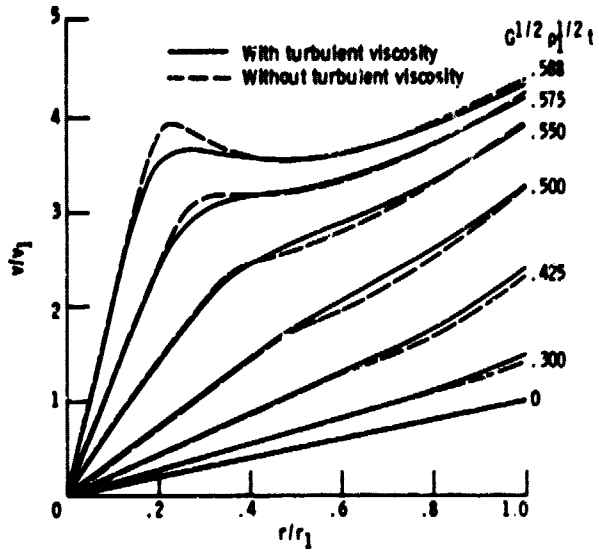

Figure 6. - Development of tangential velocity profile in vortex. $u^0/(G^{1/2}\rho_1^{1/2}) = 1$. $p_1/(G\rho_1^2 r_1^2) = 0.1$. $\gamma = 5/3$. Density and angular velocity are initially uniform, and radial and axial velocities are initially zero. Results near center of vortex are independent of pressure, polytropic exponent, and turbulent viscosity effects.

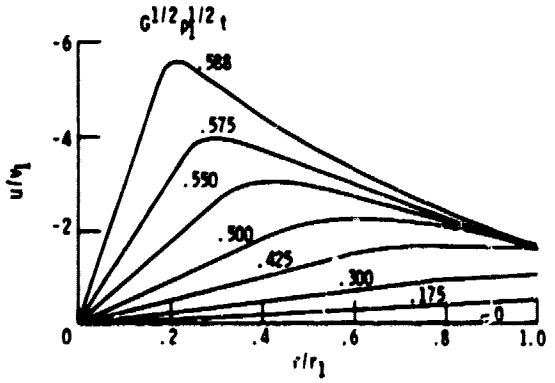

Figure 7. - Development of radial velocity profile in vortex. $u^0/(G^{1/2}\rho_1^{1/2}) = 1$. $p_1/(G\rho_1^2 r_1^2) = 0.1$. $\gamma = 5/3$. Density and angular velocity are initially uniform, and radial and axial velocities are initially zero. Results near center of vortex are independent of pressure, polytropic exponent, and turbulent viscosity effects.

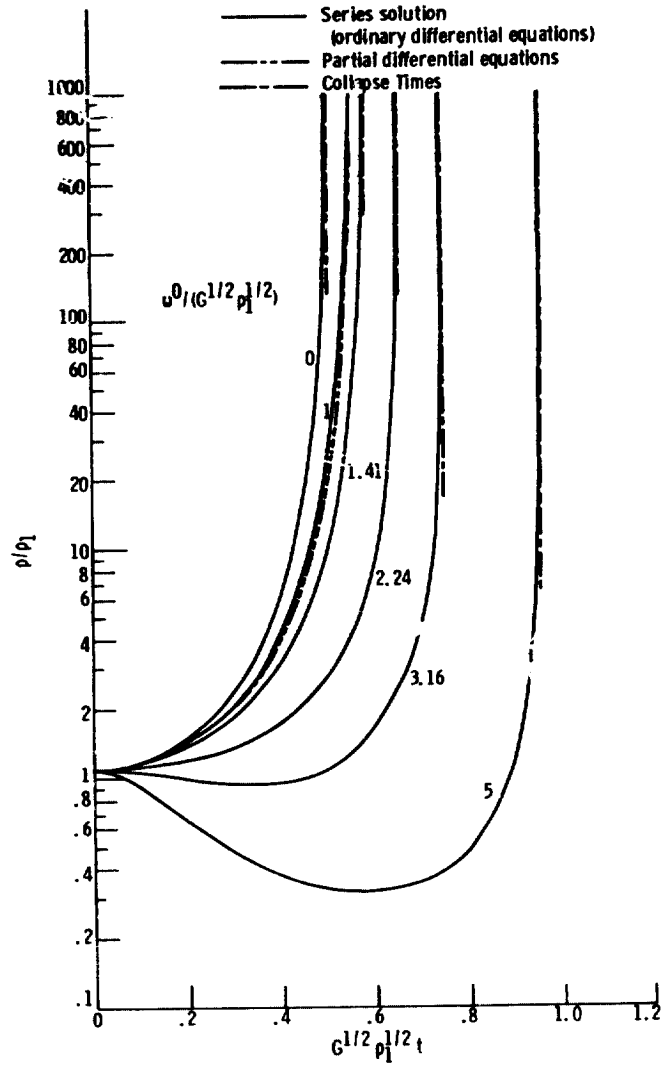

Figure 8. - Time evolution of density at center of vortex for various values of rotation parameter. $\Delta\rho^0/\rho_1 = 0.1$ and $n > 2$ in equations (45) and (46). Angular velocity near center is initially uniform, and radial and axial velocities near center are initially zero. Results are independent of pressure, polytropic exponent, and turbulent viscosity effects.

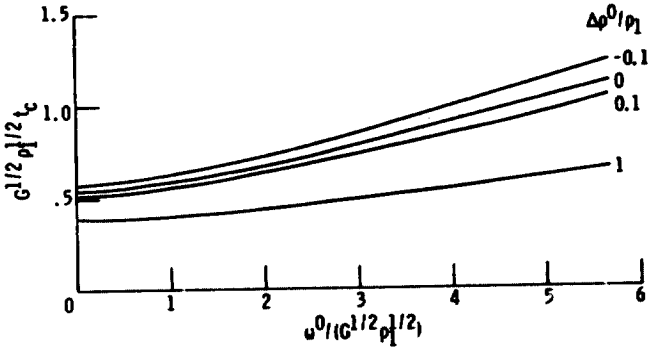

Figure 9. - Dimensionless collapse times plotted as a function of rotation parameter and initial density fluctuation. $n > 2$ in equations (45) and (46). Angular velocity near center is initially uniform, and radial and axial velocities near center are initially zero. Results are independent of pressure, polytropic exponent, and turbulent viscosity effects.

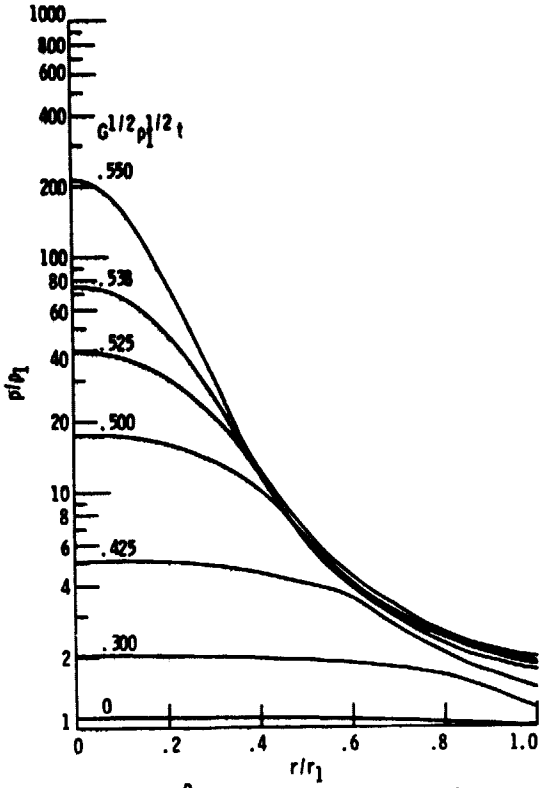

(a) $\Delta\rho^0/\rho_1 = 0.1$ in equations (45) and (46).

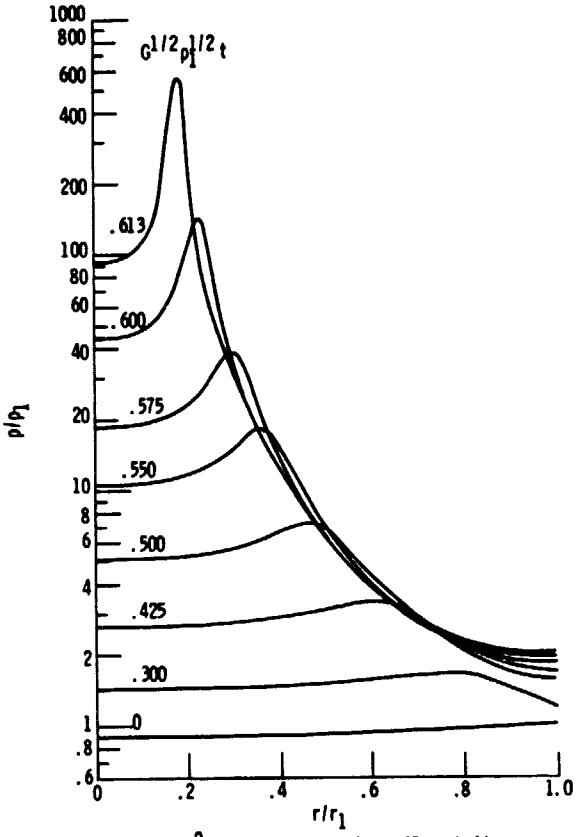

(b) $\Delta\rho^0/\rho_1 = -0.1$ in equations (45) and (46).

Figure 10. - Concluded.

Figure 10. - Development of density profile in vortex. $n = 4$ in equations (45) and (46). $\omega^0/(G^{1/2}\rho_1^{1/2}) = 1$. $p_1/(G\rho_1^2 r_1^2) = 0.1$. $\gamma = 5/3$. Angular velocity is initially uniform, and radial and axial velocities are initially zero. Results near center of vortex are independent of pressure, polytropic exponent, and turbulent viscosity effects.

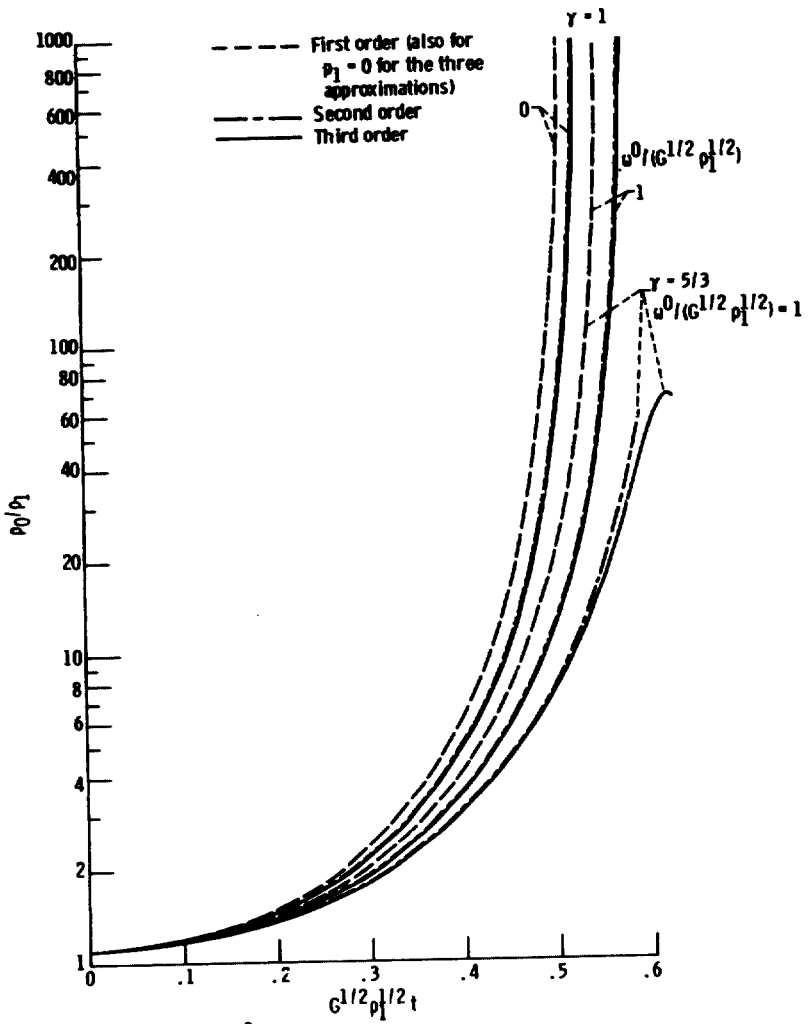

(a) $\Delta\rho^0/\rho_1 = 0.1$ in equations (45) and (46).

Figure 11. - Time evolution of density at center of vortex for n = 2 in equations (45) and (46). $\rho_1/(G\rho_1^2 r_1^2) = 1$. Angular velocity near center is initially uniform, and radial and axial velocities near center are initially zero.

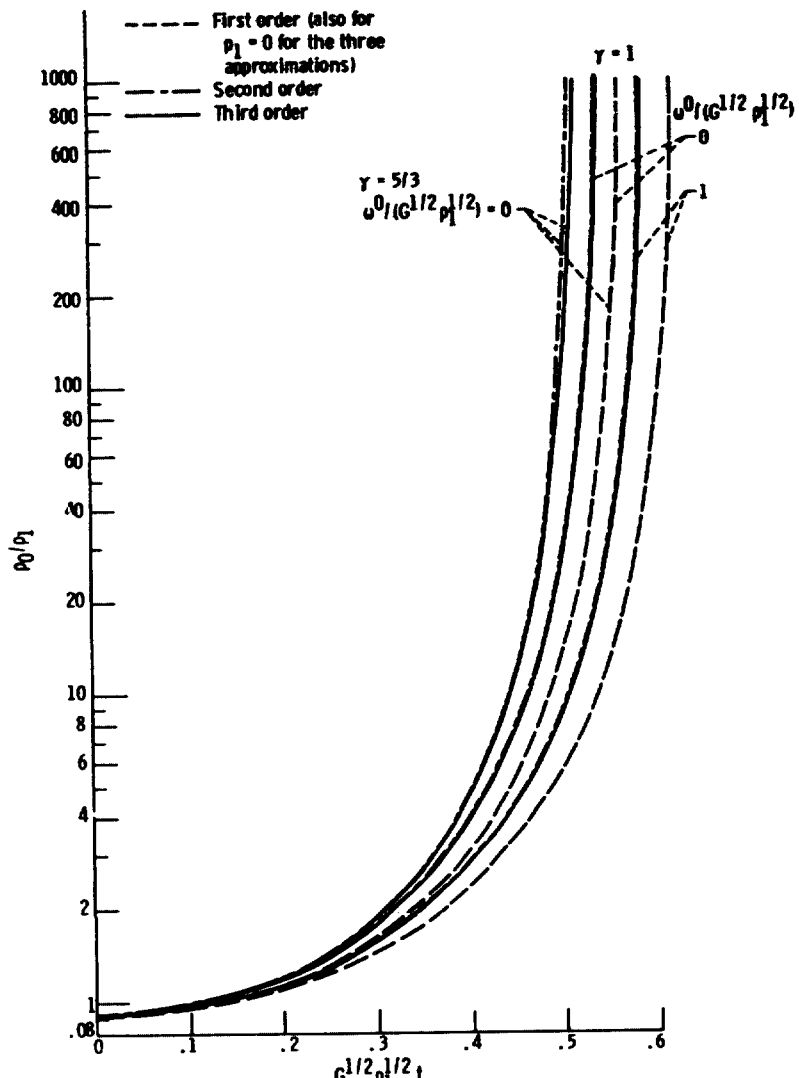

(b) $\Delta\rho^0/\rho_1 = -0.1$ in equations (45) and (46).

Figure 11. - Concluded.